Journal of Geodesy (2001) 75: 633–640

Journal of Geodesy

Accuracy of GPS-derived relative positions as a function of interstation distance and observing-session duration

M. C. Eckl, R. A. Snay, T. Soler, M. W. Cline, G. L. Mader

National Geodetic Survey, NOS, NOAA, N/NGS5, 1315 East–West Highway, Room 9115, Silver Spring, MD 20910-3282, USA
e-mail: richard.snay@noaa.gov; Tel: + 1-301-713-3202; Fax + 1-301-713-4327

Received: 5 February 2001 / Accepted: 14 May 2001

Abstract. Ten days of GPS data from 1998 were processed to determine how the accuracy of a derived three-dimensional relative position vector between GPS antennas depends on the chord distance (denoted L) between these antennas and on the duration of the GPS observing session (denoted T). It was found that the dependence of accuracy on L is negligibly small when (a) using the 'final' GPS satellite orbits disseminated by the International GPS Service, (b) fixing integer ambiguities, (c) estimating appropriate neutral-atmosphere-delay parameters, (d) 26 km $\leq L \leq$ 300 km, and (e) 4 h $\leq T \leq$ 24 h. Under these same conditions, the standard error for the relative position in the north–south dimension (denoted S_n and expressed in mm) is adequately approximated by the equation $S_n = k_n/T^{0.5}$ with $k_n = 9.5 \pm 2.1$ mm $\cdot$ h$^{0.5}$ and T expressed in hours. Similarly, the standard errors for the relative position in the east–west and in the up-down dimensions are adequately approximated by the equations $S_e = k_e/T^{0.5}$ and $S_u = k_u/T^{0.5}$, respectively, with $k_e = 9.9 \pm 3.1$ mm $\cdot$ h$^{0.5}$ and $k_u = 36.5 \pm 9.1$ mm $\cdot$ h$^{0.5}$.

Key words: GPS baseline accuracy – GPS positional time dependency accuracy – Continuously operating reference stations applications

1 Introduction

The Global Positioning System (GPS) has dramatically changed the way that surveyors, GIS/LIS professionals, engineers, and others measure positional coordinates. These practitioners can now determine the three-dimensional (3-D) coordinates of a new point with centimeter-level accuracy relative to a control point located several hundred kilometers away. That control point, moreover, may already be associated with a GPS receiver that is being continuously operated by some institution for any of several diverse applications. The National CORS (Continuously Operating Reference Stations) system (http://www.ngs.noaa.gov/CORS/) is a network of such active control points (Fig. 1).

This investigation was motivated in great part by the need to address the practicality of using the National CORS system, or some similar network of permanently mounted GPS base stations, for providing accurate positioning control. We address in this article how the accuracy of an observed 3-D relative position vector between the GPS antenna at a control point C and one at a new point P depends on the chord distance (or baseline length, denoted L) and on the duration of the observing session (or time, denoted T). We focus our study on those cases when 26 km $\leq L \leq$ 300 km, because such baseline lengths are typically encountered by GPS users who rely on the National CORS system for control (Fig. 2). Similar studies have been previously published by Davis et al. (1989), Dong and Bock (1989), Larson and Agnew (1991), Feigl et al. (1993), Schenewerk et al. (1993), and Creager and Maggio (1998). Our study extends these earlier studies by introducing mathematical expressions to quantify the dependence of accuracy on T. Also, relative to these earlier studies, our study reflects a more current picture of the improved accuracy that may be achieved due to advances in GPS technology and processing techniques.

Clearly, the final accuracy depends on several factors in addition to L and T, including the methodology and the software used for processing GPS data. Here the 'static-baseline, ionospheric-free, double differenced carrier phase' methodology as encoded in the PAGES (Program for the Adjustment of GPS Ephemerides) software was used. PAGES is an extremely flexible software package developed at the National Geodetic Survey (NGS) that may be applied to estimate several quantities in addition to relative positions among a collection of GPS antennas. In particular, PAGES may be applied to estimate GPS satellite orbits (ephemerides), site velocities, neutral atmosphere delays, and

Correspondence to: R. A. Snay

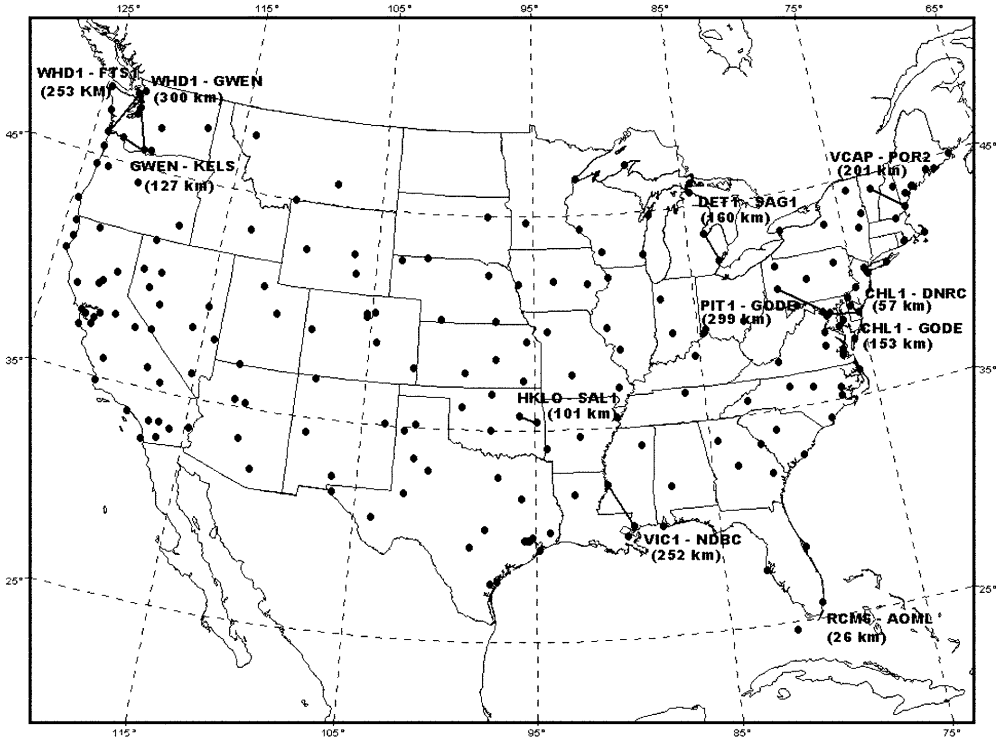

Fig. 1. That part of the National CORS network contained within the 48 contiguous states and the baselines involved in this study. Numbers denote baseline lengths (L)

ocean-loading parameters. The following section contains a general description of PAGES and identifies the options selected here for processing pertinent GPS data. Among these options, double-differenced phase ambiguities were fixed to integer values whenever possible; however, in some cases these ambiguities could be reliably fixed only if T were about 4 h or more. In this article, therefore, only cases when $4\ \text{h} \le T \le 24\ \text{h}$ were investigated.

The accuracy of an observed vector between antennas at C and P also depends on the accuracy of the auxiliary information involved in processing the GPS data. In particular, the final accuracy of the vector strongly depends on the accuracy of the GPS satellite orbits used during processing. This article exclusively uses the 'final' orbits disseminated by the International GPS Service (IGS) (http://igscb.jpl.nasa.gov/). These IGS orbits currently provide 3-D satellite positions with a standard error of about 5 cm. Our results indicate that the accuracy of an observed vector depends insignificantly on L when using such accurate orbits, meaning that a CORS located several hundred kilometers away may be effectively used for positioning control. Our results also indicate that the accuracy of an observed vector is proportional to $T^{-0.5}$ for the range of L and T considered in this article.

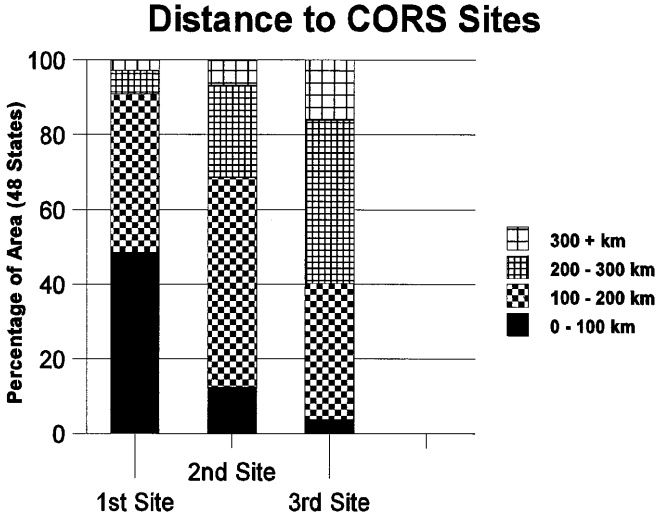

Fig. 2. Percentage of land area in the 48 contiguous states with respect to the distance to the nearest three sites in the National CORS system as of April 2001

2 Methodology and data processing

Currently over 97% of the land area of the 48 contiguous states lies within 300 km of a site in the National CORS system, and over 83% of this land area lies within 300 km of at least three such sites (Fig. 2). This coverage defined the maximum distance L for the study. A total of 19 National CORS sites distributed widely throughout the continental US were selected to form 11 baselines varying from 26 to 300 km in length. One station for each baseline was considered as the control point C (i.e. a point whose positional coordinates are already known) and the other as the 'unknown' point P (i.e. a point whose positional coordinates are unknown). For each baseline, we selected 10 days of data observed in May 1998. Each day's data were subdivided into mutually non-overlapping sessions

for each of several selected values of T (4, 6, 8, 12, and 24 h). For each subset of data, we computed the positional coordinates of P relative to the adopted positional coordinates of C. Data were processed using the version of PAGES (version 9809.21) that was current when we processed the data in 1998. All computations were performed relative to the International Terrestrial Reference Frame of 1996 (ITRF96) (Sillard et al. 1998). Previously adopted ITRF96 velocities for C and P were used to update all computed relative positions to the same date, 1 January 1999. Table 1 identifies the 11 baselines, and Table 2 designates the various observing sessions.

For each day and each unknown point P, a position was computed for each 24-h session. The average position from the ten 24-h sessions was then adopted as the 'true' position of P. For each baseline, the differences in north, east, and up (n, e, and u) from this true position were determined for every observing session. These differences form the basis for the statistics presented throughout this paper.

There are a couple of limitations associated with our study. First, because we are comparing individual GPS solutions with the average of these solutions, our study is incapable of detecting systematic differences between our GPS processing technique and other GPS processing techniques. For the same reason, our study is incapable of detecting systematic differences between GPS results and results obtained using other observational techniques, for example, electronic-distance-measurement technology, very-long-baseline interferometry, and satellite laser ranging. Hence, our derived standard errors represent the repeatability of our GPS solutions as opposed to being rigorous accuracy estimates. Second, our study is limited by the fact that it involved GPS data observed only during May 1998. Hence, seasonal effects (such as those due to large variations in temperature and humidity) are not sensed, nor are long-term effects (such as those due to large variations in solar activity). We note that solar activity during 1998 was relatively low.

As mentioned previously, all GPS data involved in this study were processed using PAGES. NGS personnel also use PAGES routinely to estimate parameters characterizing GPS satellite orbits and Earth-orientation. In addition, NGS personnel use PAGES to process National CORS data on a daily basis for deriving pertinent site coordinates and for assessing data quality (http://www.ngs.noaa.gov/CORS/). Also, many scientists use PAGES to calculate relative positions among a set of sites at which GPS data have been collected simultaneously over some time interval. Other applications of PAGES include the estimation of site velocities, ocean-loading parameters, and neutral-atmospheric-delay parameters. These and other applications require PAGES to be both rigorous and flexible in addressing the various systematic errors that contaminate GPS observations. Here we discuss features of PAGES that are relevant to our study. Readers may find a comprehensive documentation of PAGES, together with tutorial material, at http://www.ngs.noaa.gov/GRD/GPS/DOC/pages/pages.html.

Table 1. Schedule of observations

Baseline[b]	L (km)	Day of year (1998)[a]																
		121	122	123	124	125	126	127	128	129	130	131	132	133	134	135	136	137
RCM6 → AOML	26								X	X	X	X	X	X	X	X	X	X
CHL1 → DNRC	57	X	X	X	X	X	X	X	X	X	X							
HKLO → SAL1	101	X	X	X	X	X	X	X	X	X	X							
GWEN → KELS	127	X	X	X	X	X	X	X	X	X	X							
CHL1 → GODE	153	X	X	X	X	X	X	X	X	X	X							
DET1 → SAG1	160	X			X	X	X	X	X	X	X		X	X				
VCAP → POR2	201	X	X	X	X	X	X	X	X	X	X							
VIC1 → NDBC	252	X	X	X	X	X	X	X	X	X	X							
WHD1 → FTS1	253	X	X	X	X	X	X			X	X	X	X					
PIT1 → GODE	299	X	X	X	X		X	X	X	X	X		X					
WHD1 → GWEN	300	X	X	X	X	X	X	X	X	X	X							

[a] 'X' indicates that data from this day were included in the study
[b] The coordinates of the first station ('hub') of each pair were held 'fixed' while the coordinates of the second station were 'solved for'

Table 2. Session designations[a]

Session length (h)	Sessions/occupation times						Sessions
	a	b	c	d	e	f	
4	0000–0400	0400–0800	0800–1200	1200–1600	1600–2000	2000–2400	6
6	0000–0600	0600–1200	1200–1800	1800–2400			4
8	0000–0800	0800–1600	1600–2400				3
12	0000–1200	1200–2400					2
24	0000–2400						1

[a] For 10 days and 11 baselines, there are a total of 660 4-h, 440 6-h, 330 8-h, 220 12-h, and 110 24-h sessions

PAGES employs an LS process using observed phases of the L1 and L2 carrier frequencies to estimate the various parameters identified in the previous paragraph. In this investigation a 30-s sampling rate was used because phase measurements were nominally recorded at this rate for most CORS sites involved in this study. Similar results may have been obtained by processing the data with a slower sampling rate, but the 30-s sampling rate would allow the editing algorithms encoded in the PAGES suite of programs to detect data problems more effectively than any slower rate. We would, however, have opted to process using a faster sampling rate, had the GPS receivers recorded the phase measurements at such a rate, simply to enable more effective data snooping.

In applying PAGES, we chose to ignore all phase measurements corresponding to epochs when satellite elevation angles were less than 15°. Studies by Elósegui et al. (1995) and Jaldehag et al. (1996) reveal that relative positions, especially in the vertical dimension, depend on the choice of the cutoff elevation angle, and so the NGS has adopted the convention of using 15° as the default cutoff elevation angle for all CORS-related processing. PAGES also accounts for antenna-phase-center variation which if ignored could introduce up to a 10-cm error in height when processing GPS data for a baseline involving two different antenna types (see Mader and MacKay 1996; Meertens et al. 1996; Rothacher and Schär 1996).

In this study we deal with only one pair of GPS receivers at a time, although PAGES is capable of rigorously processing data collected simultaneously from many tens of GPS receivers. For each data epoch and for each carrier frequency (L1 and L2), the software forms pairs of sites and pairs of satellites to compute double-differenced values of the measured phases. The site pairs and the satellite pairs are so chosen that the set of double-differenced values are mathematically non-redundant. This differencing eliminates timing errors associated with both the satellite clocks and the receiver clocks.

Solutions were determined using the so-called ion-free linear combination of the double-differenced L1 and L2 carrier-phase values. This action removes first-order ionospheric refraction effects on the GPS signal. Furthermore, the PAGES feature that sets double-differenced L1 and L2 phase ambiguities to integer values whenever possible was enforced. This action reduces the number of unknown parameters that have to be estimated via the LS process embodied in PAGES. Hence, if these ambiguities have been set to their correct integer values, then the remaining parameters can be estimated with greater precision. Our experience suggests that PAGES reliably set these ambiguities to integer values for all baselines involved in this study when $T \geq 4$ h.

Finally, solutions were obtained using the PAGES feature that enables users to estimate, for each site, a set of parameters that characterizes the time-dependent effects of the neutral atmospheric delay on phase measurements recorded at that site. Each site-specific set includes an unknown parameter at the beginning of the observing session and another after each 2-h increment, with the stipulation that PAGES would linearly interpolate the estimated bi-hourly values of these parameters to obtain appropriate values for data epochs recorded during the observing session.

3 Resulting statistics

For each baseline and for each considered value of T (4, 6, 8, 12, and 24 h), the various estimates for the positional coordinates of the 'unknown' points were compared with our derived 'true' coordinates of these points, and the corresponding differences were resolved into north (n), east (e), and up (u) components. RMS values in each component were then computed for each baseline and each value of T. Any individual component of a positional difference that exceeded its corresponding RMS value by more than a factor of three was then discarded and the corresponding RMS value was recomputed. Table 3 presents these recomputed RMS values. Overall 3.3% of the 4-h sessions were discarded, 3.1% of the 6-h sessions, 2.5% of the 8-h sessions, 0.4% of the 12-h sessions, and 0.0% of the 24-h sessions.

Figures 3, 4, and 5 present our derived statistics graphically. Figure 3 comprises a set of scatter plots that display the distribution of positional differences for each dimension, each baseline, and each value of T. Figure 4 shows how computed RMS values vary as a function of L, and Fig. 5 shows how computed RMS values vary as a function of T. These three figures reveal that, as expected, the RMS (or scatter) in the up direction is larger than that in either of the horizontal components (n or e). Also as expected, these figures indicate that RMS decreases as T increases. Somewhat unexpectedly, however, the figures suggest that the computed RMS values do not vary significantly as a function of L. We address these results in greater detail in the next section after developing plausible equations for characterizing accuracy as a function of L and T.

4 Accuracy dependency analysis

Let $S_n(L,T)$ correspond to the standard error in the north–south direction as a function of L and T. We assume that $S_n(L,T)$ may be adequately represented by an equation of the form

$$S_n(L,T) = [a_n/T + b_n L^2/T + c_n + d_n L^2]^{0.5} \quad (1)$$

where a_n, b_n, c_n, and d_n are constants. That is, we assume that the variance $[S_n(L,T)]^2$ can be represented as the sum of four independent error terms. The error terms involving a_n and b_n are proportional to the reciprocal of T, whereas those involving c_n and d_n are independent of T. The error terms involving b_n and d_n are proportional to L^2, whereas those involving a_n and c_n are independent of L^2.

Equations of the same form were assumed to represent $S_e(L,T)$ and $S_u(L,T)$, the standard errors in the east–west direction and in the up–down (vertical)

direction, respectively. Now assuming that the RMS values contained in Table 3 closely approximate corresponding standard errors, we used these tabulated values to compute LS estimates for the constants: a_n, b_n, c_n, d_n, a_e, b_e, c_e, d_e, a_u, b_u, c_u, and d_u. Our estimated values are given in Table 4. Also, the last column of Table 4 displays the ratio of each estimate to its corresponding formal 1-sigma uncertainty. These ratios indicate that only the estimates for a_n, a_e, and a_u differ statistically from zero at the 95% confidence level. Hence, for characterizing our experimental results, Eq. (1) may be effectively replaced by

Table 3. RMS values (mm) of n, e, and u for each baseline and each value of T

		26 km	57 km	101 km	127 km	153 km	160 km	201 km	252 km	253 km	299 km	300 km	Mean
4-h	RMS n	3.8	5.6	4.4	4.8	3.5	5.0	6.3	4.1	5.7	4.1	4.9	4.7
	RMS e	4.1	4.1	4.7	4.0	4.3	4.3	4.7	5.8	9.3	4.0	6.0	5.0
	RMS u	12.7	19.7	20.1	12.7	16.0	18.4	23.9	22.9	18.2	14.7	15.9	17.7
6-h	RMS n	2.8	5.3	2.9	3.7	4.0	4.0	5.0	4.1	3.5	3.3	3.5	3.8
	RMS e	3.4	3.5	3.5	2.8	4.5	3.4	2.8	4.3	3.6	3.8	4.5	3.6
	RMS u	9.0	12.5	17.2	11.4	15.3	15.0	18.6	18.5	10.6	13.6	14.4	14.2
8-h	RMS n	2.6	3.2	3.6	3.4	2.0	2.8	3.6	3.3	3.2	2.7	3.7	3.1
	RMS e	2.8	2.7	2.2	2.2	2.8	2.8	3.5	3.4	4.9	2.1	3.3	3.0
	RMS u	6.7	11.2	12.9	10.8	15.2	12.2	21.9	12.5	13.0	15.5	11.2	13.0
12-h	RMS n	2.5	3.5	2.6	2.6	1.9	2.3	3.7	2.9	3.3	2.0	2.3	2.7
	RMS e	2.5	2.7	2.0	1.6	2.5	2.2	2.2	2.8	5.7	2.1	4.0	2.8
	RMS u	6.5	9.9	11.0	5.6	12.6	8.4	14.8	13.8	10.3	12.0	7.8	10.2
24-h	RMS n	1.4	1.6	2.1	1.5	1.6	2.8	1.9	2.0	1.6	1.5	0.9	1.7
	RMS e	1.4	2.1	2.5	1.5	1.7	1.5	1.8	1.2	3.7	1.4	3.0	2.0
	RMS u	4.7	6.1	9.5	4.3	11.9	11.6	11.7	8.3	3.2	10.0	6.9	8.0

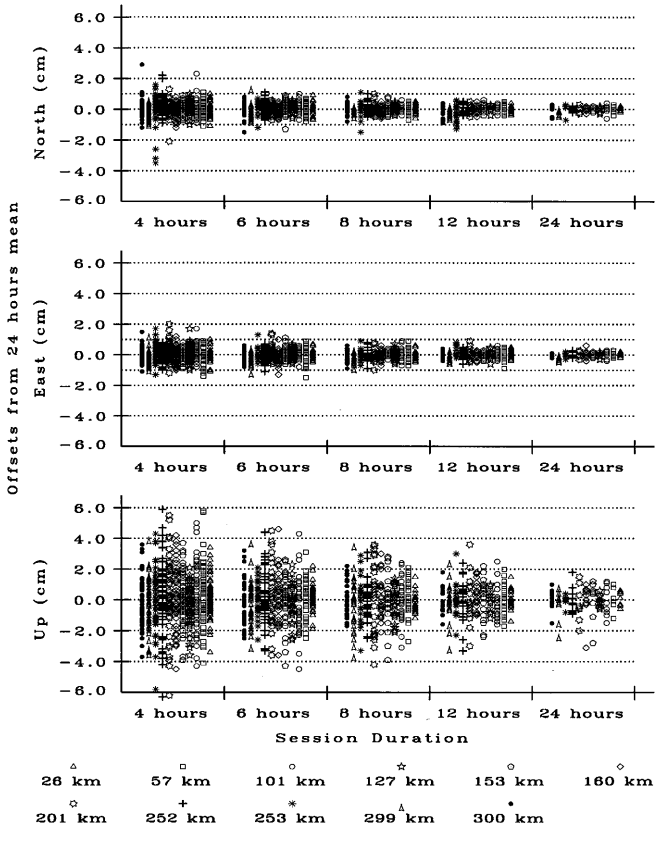

Fig. 3. Distribution of differences between estimated positions of the 'unknown' points and their corresponding 'true' positions. Each horizontal axis is partitioned into five blocks with each block representing a selected value of T. Within each block there are 11 stacks of positional differences with each stack representing a particular baseline

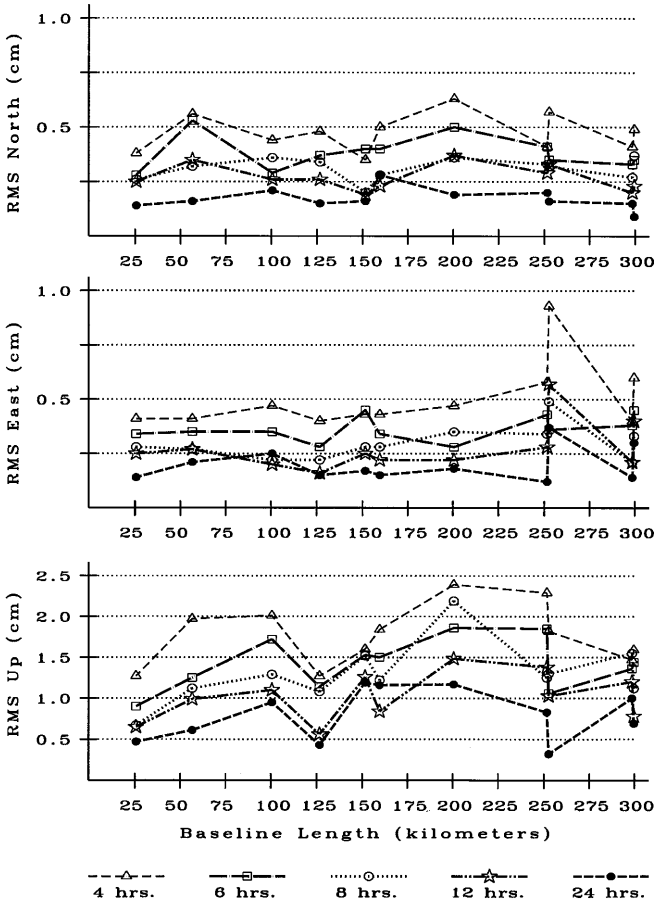

Fig. 4. RMS values for each baseline and each value of T. Each line in the above graphs connects RMS values sharing a common value for T. Note that the vertical scale of the bottom graph differs from that of the other two graphs

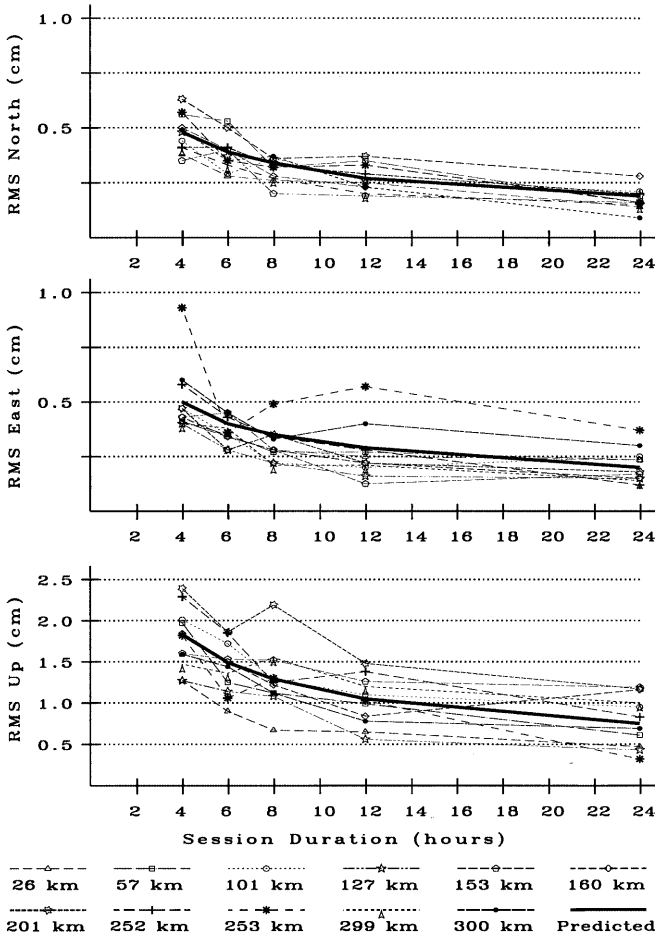

Fig. 5. Each *thin line* connects RMS values for a particular baseline. Bold lines represent RMS values predicted by the equations derived in this paper. Note that the vertical scale of the bottom graph differs from that of the other two graphs

$$S_n(L,T) = [a_n/T]^{0.5} \tag{2}$$

or equivalently

$$S_n(L,T) = k_n/T^{0.5} \tag{3}$$

with similar equations for $S_e(L,T)$ and $S_u(L,T)$.

Now using Eq. (3) and the RMS values given in Table 3, we obtained the following LS estimates:

$$\begin{aligned} k_n &= 9.5 \pm 2.1\,\text{mm} \cdot \text{h}^{0.5} \\ k_e &= 9.9 \pm 3.1\,\text{mm} \cdot \text{h}^{0.5} \\ k_u &= 36.5 \pm 9.1\,\text{mm} \cdot \text{h}^{0.5} \end{aligned} \tag{4}$$

The bold lines in Fig. 5 represent standard errors (or RMS values) that were computed using these estimates for the parameters in their respective equations. Figure 5, consequently, enables readers to visually compare predicted RMS values with the empirically derived RMS values. Table 5 compares values computed from these equations with the mean RMS values for all 11 baselines for each dimension and each value of T. Figure 5 and Table 5, hence, render a sense of the uncertainty associated with our estimates for k_n, k_e, and k_u. Formal

Table 4. Estimated values of constants in Eq. (1)

Parameter (units)	Estimated value	Formal 1-sigma uncertainty	Ratio
a_n (mm^2 · h)	92.60	15.53	5.96
a_e (mm^2 · h)	70.24	29.69	2.37
a_u (mm^2 · h)	1209.10	280.07	4.32
b_n (ppb^2 · h)	84.78	311.05	0.28
b_e (ppb^2 · h)	935.43	594.59	1.57
b_u (ppb^2 · h)	268.81	5608.34	0.05
c_n (mm^2)	−0.29	2.35	−0.12
c_e (mm^2)	−0.83	4.50	−0.18
c_u (mm^2)	4.22	42.40	0.10
d_n (ppb^2)	−17.99	47.09	−0.38
d_e (ppb^2)	−15.43	90.01	−0.17
d_u (ppb^2)	372.12	849.00	0.44

Table 5. Mean RMS (mm) for all 11 baselines

T (h)	North (S_n)	East (S_e)	Up (S_u)
4	4.7 (4.8)	5.0 (5.0)	17.7 (18.2)
6	3.8 (3.9)	3.6 (4.0)	14.2 (14.9)
8	3.1 (3.4)	3.0 (3.5)	13.0 (12.9)
12	2.7 (2.7)	2.8 (2.9)	10.2 (10.5)
24	1.7 (1.9)	2.0 (2.0)	8.0 (7.5)

Parentheses contain values predicted by the equations, $S_n = 9.5/T^{0.5}$, $S_e = 9.9/T^{0.5}$, and $S_u = 36.5/T^{0.5}$

1-sigma uncertainties associated with these estimated parameters are given in Eq. (4). These uncertainties indicate, in part, the permissible range of values that would be obtained if we were to repeat our experiment using 11 different baselines and/or some other 10 days of data. In this respect, we could have estimated k_n, k_e, and k_u more precisely simply by involving more baselines and/or more days of data in our experiment. There is a limit, however, to how precisely we can estimate these three parameters because part of the uncertainty corresponds to the adequacy (or inadequacy) of using Eq. (3) to express baseline accuracy. Perhaps a more complex mathematical expression involving additional parameters is warranted. In addition to L, such parameters may include the geographic location of the baseline and the type of GPS hardware at each site. Also, perhaps the dependence on T may be better represented by a more complex mathematical expression. Our results thus represent only some part of the journey towards fully understanding baseline accuracy.

Note that our experiment justifies the use of Eq. (3) only for those values of T between 4 and 24 h. While we feel that this equation may be extrapolated with reasonable confidence for $T > 24$ h, other experiments conducted by us indicate that Eq. (3) does not apply for $T < 4$ h. These other experiments are inconclusive, however, because we encountered cases when PAGES was unable to reliably fix phase ambiguities to integer values in the automated mode when $T < 4$ h. Hence, we have opted to study alternative algorithms for so fixing phase ambiguities before publishing standard errors for baseline vectors when $T < 4$ h.

5 Discussion

The fact that our estimates for c_n, c_e, and c_u do not statistically differ from zero at the 95% confidence level implies that estimated relative positions approach their 'true' values as T approaches infinity. Because our 'true' values correspond to means derived from the GPS data used in this study, this result is as expected. Non-zero estimates for c_n, c_e, and c_u may have resulted, had we derived 'true' values from some alternative source of data.

The fact that our estimates for b_n, d_n, b_e, d_e, b_u, and d_u do not statistically differ from zero at the 95% confidence level implies that the dependency of positioning accuracy on L is so slight that it is below the threshold associated with our experiment. Note that we are not saying that positioning accuracy is independent of L, but that this dependency is negligibly small.

Other investigators (Dong and Bock 1989; Larson and Agnew 1991; Feigl et al. 1993) have used the equation

$$S_n(L, T = 7\,\mathrm{h}) = p_n + q_n L \tag{5}$$

and similar equations for $S_e(L,\ T = 7\ \mathrm{h})$ and $S_u(L,\ T = 7\ \mathrm{h})$ to study the dependency of accuracy on L for $L < 500$ km. As the observations for their experiments were conducted before 1992, the then existing GPS satellite constellation afforded adequate coverage for only about a 7-hour window. Hence, for their experiments, T remained essentially constant at a value of approximately 7 hours. These investigators published values for q_n in the range from 2 to 12 parts per billion (ppb), for q_e in the range from 5 to 28 ppb, and for q_u in the range from −11 to 130 ppb. For comparison, we used the data in Table 3 corresponding to $T = 6$ h and $T = 8$ h and obtained the following estimates:

$$p_n = 3.4 \pm 0.4\,\mathrm{mm} \quad q_n = 0.4 \pm 1.8\,\mathrm{ppb}$$
$$p_e = 2.8 \pm 0.4\,\mathrm{mm} \quad q_e = 3.0 \pm 1.7\,\mathrm{ppb}$$
$$p_u = 11.1 \pm 1.5\,\mathrm{mm} \quad q_u = 14.0 \pm 7.8\,\mathrm{ppb}$$

where our uncertainties correspond to formal 1-sigma values. Our estimates for q_n, q_e, and q_u tend toward the low side of those published by the other investigators, likely reflecting improvements in GPS technology and processing techniques between the 1986–1992 time frame (when these other investigators conducted their experiments) and the 1998–1999 time frame (when we conducted our experiments). For the earlier studies, for example, people did not have access to precomputed precise satellite orbits, as are now available from the IGS. More to the point, however, our estimates for q_n, q_e, and q_u do not statistically differ from 0 ppb at the 95% confidence level. This result further corroborates our earlier statement that the dependency of accuracy on L is negligibly small. Note that for $L = 300$ km, 1 ppb would correspond to 0.3 mm.

The results of our study indicate that highly accurate positional coordinates can be obtained using CORS as control even though the distance to the nearest CORS may be several hundred kilometers. One drawback, however, is the need for rather long observing sessions to realize these accuracies. It is costly to remain at a single site for several hours, and this cost may be prohibitive if several tens of sites need to be positioned. A remedy, however, is available if two or more GPS receivers are available and if the points to be positioned are clustered within a few km of a site where one of these receivers can be placed as a local base ('hub') station. This scenario would allow the remaining GPS receivers to accurately position the various new points relative to the hub station by spending a relatively short time at each new point. Meanwhile, the GPS data being collected at the hub station can also be used to accurately position this base station relative to one or more existing CORS. Consequently, all visited points can be effectively positioned relative to the CORS network.

Cases will exist, nevertheless, when only a single dual-frequency GPS receiver is available and/or the points to be positioned are widely separated. For these cases, it is not unreasonable that technology will sufficiently improve in the near future to enable accurate positioning over long distances with observing sessions of under an hour. Towards this objective, scientists at the National Oceanic and Atmospheric Administration (NOAA) are investigating the use of NOAA-generated weather models to improve current procedures for addressing the weather-related errors that contaminate GPS observations (Marshall et al. 2001).

As previously mentioned, we used the 'final' satellite orbits disseminated by the IGS for processing the GPS data involved in this study. IGS 'final' orbits for a given day are available about 2 weeks after that day. Currently, these orbits provide 3-D satellite positions with a standard error of 5 cm (http://igscb.jpl.nasa.gov/). If we had used less accurate orbits, then each of the quantities $S_n(L,T)$, $S_e(L,T)$, and $S_u(L,T)$ (for a fixed value of L and T) would have increased (Leick, 1995, pp 275–277). Some applications, however, require more timely processing of observed GPS data. For such applications, the IGS disseminates 'rapid' orbits that are available in 2 days and provide 3-D satellite positions with a standard error of 10 cm (http://igscb.jpl.nasa.gov/). For processing GPS data in real time, both the IGS and the US Department of Defense (DoD) provide orbits that predict satellite locations for several hours beyond the time when the orbits were generated. The DoD-predicted orbits are commonly referred to as the 'broadcast' orbits, as DoD uploads these orbits to the GPS satellites whereupon the satellites broadcast these orbits as part of the GPS signal. DoD-predicted orbits provide 3-D satellite positions with a standard error of about 2.7 m (Springer and Hugentobler 2001). The IGS-predicted orbits, referred to as the 'ultra-rapid' orbits, are available via the Internet and provide 3-D satellite positions with a standard error in the 30- to 40-cm range (Springer and Hugentobler 2001).

In this article we have discussed only the accuracy associated with measuring the relative position vector between two GPS antennas. The total error involved in

positioning a 'point-of-interest' using CORS as control will also depend both on the accuracy of the CORS coordinates and on the accuracy of the offset measurements that relate the 'point-of-interest' to its associated GPS antenna. To help mitigate errors associated with CORS coordinates, we recommend that the point-of-interest be positioned in a statistical manner relative to two or more CORS sites. For example, perform a network adjustment involving each baseline connecting the point-of-interest to a distinct CORS site, and (in this adjustment) constrain the coordinates for these CORS sites to their adopted values.

6 Summary

We processed several sets of GPS data for 11 baselines, each connecting a pair of sites contained in the National CORS network, to determine how the accuracy of a GPS-derived 3-D relative position vector between GPS antennas depends on L and T. This study was restricted to values of L ranging between 26 and 300 km and to values of T ranging between 4 and 24 h. The data were processed with the PAGES software using the 'final' GPS satellite orbits disseminated by the IGS, fixing integer ambiguities when possible, and estimating appropriate neutral-atmosphere-delay parameters. Under these conditions, it was found that the dependency of accuracy on L is negligibly small. Moreover, the following equations were found to adequately quantify this accuracy as a function of T only:

$$S_n = k_n/T^{0.5} \quad S_e = k_e/T^{0.5} \quad S_u = k_u/T^{0.5}$$

where S_n, S_e, and S_u are expressed in mm; T is expressed in hours; and

$$k_n = 9.5 \pm 2.1\,\text{mm} \cdot h^{0.5}, \quad k_e = 9.9 \pm 3.1\,\text{mm} \cdot h^{0.5},$$
$$k_u = 36.5 \pm 9.1\,\text{mm} \cdot h^{0.5}$$

These empirically determined results indicate that the magnitude of the positional errors along the horizontal components are about equal and the error associated with the vertical component is about 3.6 times that of the horizontal error.

Acknowledgements. We thank our NGS colleagues for their assistance in performing this study and in preparing this article. We particularly wish to acknowledge the contributions of Juliana Blackwell, Cindra Craig, Nancy Doyle, Richard Foote, Lucy Hall, Stephen Hilla, Dennis Milbert, Mark Schenewerk, and Neil Weston. We are also thankful for helpful suggestions from two anonymous reviewers.

References

Creager GJ, Maggio RC (1998) How long must we wait? Duration of GPS observations for long GPS baselines. Proc Navigation's 54th Annual Meeting, Denver, pp 467–475

Davis JL, Prescott WH, Svarc J, Wendt K (1989) Assessment of Global Positioning System measurements for studies of crustal deformation. J Geophys Res 94(B13): 13 635–13 650

Dong DN, Bock Y (1989) Global Positioning System network analysis with phase ambiguity resolution applied to crustal deformation studies in California. J Geophys Res 94(B4): 3949–3966

Elósegui P, Davis JL, Jaldehag RTK, Johansson JM, Niell AE, Shapiro II (1995) Geodesy using the Global Positioning System: the effects of signal scattering on estimates of site position. J Geophys Res 100(B6): 9921–9934

Feigl KL, Agnew DC, Bock Y, Dong D, Donellan A, Hager BH, Herring TA, Jackson DD, Jordan TH, King RW, Larsen S, Larson KM, Murray MH, Shen ZK, Webb FH (1993) Space geodetic measurement of crustal deformation in central and southern California, 1984–1992. J Geophys Res 98(B12): 21 677–21 712

Jaldehag RTK, Johansson JM, Rönnäng BO, Elósegui P, Davis JL, Shapiro II, Niell AE (1996) Geodesy using the Swedish permanent GPS network: effects of signal scattering on estimates of relative site positions. J Geophys Res 101 (B8): 17 841–17 860

Larson KM, Agnew DC (1991) Application of the global positioning system to crustal deformation measurement, 1, Precision and accuracy. J Geophys Res 96(B10): 16 547–16 565

Leick A (1995) GPS Satellite Surveying (2nd edn). John Wiley, New York

Mader GL, MacKay J (1996) Calibration of GPS antennas. In: Neilan RE, van Scoy PA, Zumberge JF (eds) Proc IGS Analysis Center Workshop, Silver Spring, MD, 19–21 March. Jet Propulsion Laboratory, Pasadena, pp 81–105

Marshall J, Schenewerk M, Snay R, Gutman S (2001) The effect of the MAPS weather model on GPS-determined ellipsoidal heights. GPS Solut 5(1): 1–14

Meertens C, Albert C, Braun J, Rocken C, Stephens B, Ware R, Exter M, Kolesnikoff P (1996) Field and anechoic chamber tests of GPS antennas. In: Neilan RE, van Scoy PA, Zumberge JF (eds) Proc IGS Analysis Center Workshop, Silver Spring, MD, 19–21 March. Jet Propulsion Laboratory, Pasadena, pp 107–118

Rothacher M, Schär S (1996) Antenna phase center offset and variations estimated from GPS data. In: Neilan RE, van Scoy PA, Zumberge JF (eds) Proc IGS Analysis Center Workshop, Silver Spring MD, 19–21 March. Jet Propulsion Laboratory, Pasadena, pp 321–326

Schenewerk M, MacKay JR, Kass W, Chin M, Mader G (1993) Rapid turnaround GPS ephemerides from the National Geodetic Survey. Proc ION GPS-93, Institute of Navigation, Alexandria, VA, pp 247–255

Sillard P, Altamimi Z, Boucher C (1998) The ITRF96 realization and its associated velocity field. Geophys Res Lett 25(17): 3223–3226

Springer TA, Hugentobler U (2001) IGS ultra rapid products for (near-) real-time applications. Phys Chem Earth 26 (6–8): 623–628